Quantitative analysis of the EGF receptor autocrine system reveals cryptic regulation of cell response by ligand capture

Ann E. DeWitt[1], Jian Ying Dong[2], H. Steven Wiley[3] and Douglas A. Lauffenburger[1,4,*]

[1]Department of Chemical Engineering, Massachusetts Institute of Technology, Cambridge, MA 02139, USA
[2]Newborn Medicine, Children's Hospital, Boston, MA 02115, USA
[3]Fundamental Sciences Division, Pacific Northwest National Laboratory, Richland, WA 99352, USA
[4]Division of Bioengineering and Environmental Health and Center for Cancer Research, Massachusetts Institute of Technology, Cambridge, MA 02139, USA
*Author for correspondence (e-mail: lauffen@mit.edu)

Accepted 29 March 2001
Journal of Cell Science 114, 2301-2313 © The Company of Biologists Ltd

SUMMARY

Autocrine signaling is important in normal tissue physiology as well as pathological conditions. It is difficult to analyze these systems, however, because they are both self-contained and recursive. To understand how parameters such as ligand production and receptor expression influence autocrine activity, we investigated a human epidermal growth factor/epidermal growth factor receptor (EGF/EGFR) loop engineered into mouse B82 fibroblasts. We varied the level of ligand production using the tet-off expression system and used metalloprotease inhibitors to modulate ligand release. Receptor expression was varied using antagonistic blocking antibodies. We compared autocrine ligand release with receptor activation using a microphysiometer-based assay and analyzed our data using a quantitative model of ligand release and receptor dynamics. We found that the activity of our autocrine system could be described in terms of a simple ratio between the rate of ligand production (V_{LT}) and the rate of receptor production (V_R). At a V_{LT}/V_R ratio of <0.3, essentially no ligand was found in the extracellular medium, but a significant number of cell receptors (30-40%) were occupied. As the V_{LT}/V_R ratio increased from 0.3 towards unity, receptor occupancy increased and significant amounts of ligand appeared in the medium. Above a V_{LT}/V_R ratio of 1.0, receptor occupancy approached saturation and most of the released ligand was lost into the medium. Analysis of human mammary epithelial cells showed that a V_{LT}/V_R ratio of $<5\times10^{-4}$ was sufficient to evoke >20% of a maximal proliferative response. This demonstrates that natural autocrine systems can be active even when no ligand appears in the extracellular medium.

Key words: Autocrine, EGF, Computational model

INTRODUCTION

Autocrine signaling was first described two decades ago as a partner to tumorigenic phenomena (Sporn and Todaro, 1980). In this mode of signaling, cells make both a receptor and the ligand that activates the receptor. Although originally envisioned as a pathological phenomenon, autocrine regulation is now recognized as a mechanism that can regulate cell responses under many different physiological conditions. These include prostate epithelial development (Kim et al., 1999), mammary epithelial development (Li et al., 1992; Wang et al., 1994; Wojcik et al., 1999), immune cell proliferation (Boussiotis et al., 1994; Duprez et al., 1985), tissue response to injury (Campochiaro et al., 1994; Piepkorn et al., 1998; Sporn and Roberts, 1992) and liver regeneration (Bissell et al., 1995; Hioki et al., 1996; Russell et al., 1993). More recently, autocrine signaling has been identified as a major mechanism of receptor cross-talk or 'transactivation'. In these cases, induction of one receptor system induces the release of an autocrine factor that activates a second type of receptor. Although the physiological significance of transactivation is unclear, it is thought to act as a mechanism to integrate information from multiple receptor systems (Hackel et al., 1999).

A prominent example of autocrine signaling is the EGF receptor (EGFR) system. Several different ligands bind to the EGFR including EGF (Carpenter and Wahl, 1990), transforming growth factor α (TGF-α) (Derynck, 1992), amphiregulin (Shoyab et al., 1989), heparin-binding EGF-like growth factor (HB-EGF) (Higashiyama et al., 1991), betacellulin (Shing et al., 1993), and epiregulin (Toyoda et al., 1995). Most cells that depend on the EGFR for proliferation and differentiation also make one or more of the cognate ligands. The EGFR system can be involved in both disease and normal tissue homeostasis, depending on the expression levels of both ligand and receptor. For example, whereas mice knockouts of EGFR show epithelial defects and multi-organ failure (Miettinen et al., 1995; Sibilia and Wagner, 1995; Threadgill et al., 1995), over-expression of EGFR ligands can induce liver and mammary tumor formation (Jhappan et al., 1990; Sandgren et al., 1990).

Although autocrine signaling is an important regulator of cell

function, it is difficult to study. This is because of both its recursive nature and the spatial limits of the autocrine loop itself. Autocrine factors, such as TGF-α, can enhance self-release through the MAPK pathway and can enhance expression of multiple ligands as well as the EGFR (Barnard et al., 1994; Fan and Derynck, 1999). The loop itself can be restricted spatially in that autocrine ligands are generally not found in the extracellular environment unless the receptors are first blocked (Dempsey and Coffey, 1994). In the case of polarized epithelial cells, TGF-α and EGFR are targeted to the basolateral surface, whereas EGF accumulates at the apical surface (Dempsey and Coffey, 1994; Dempsey et al., 1997). The importance of the spatial localization of autocrine signaling loops has been demonstrated in two model organisms of developmental biology, *Caenorhabditis elegans* (Kaech et al., 1998; Kim, 1997; Kornfeld, 1997) and *Drosophila* (Bier, 1998; Golembo et al., 1996). In vitro systems have also shown that restriction in the spatial domain of autocrine signaling is important in cellular responses (Dempsey and Coffey, 1994; Wiley et al., 1998; Will et al., 1995). For example, removing the transmembrane region of EGF in human mammary epithelial cells leads to the disruption of mammary epithelial cell organization due to a shift from autocrine to intracrine signaling (Wiley et al., 1998).

The spatial operation of an autocrine loop is also influenced by the structure of the ligand. For example, each ligand of the EGF family is initially produced as a transmembrane protein that is released by proteolysis at the cell surface. All EGF family ligands consist of a conserved receptor-binding core domain flanked on the carboxy side by a membrane-spanning domain and on the amino side by a highly variable extracellular extension (Massague and Pandiella, 1993). These extensions can be proteolytically removed prior to release of the ligand, such as the case with TGF-α (Derynck, 1992). In the case of other family members, such as HB-EGF, most of the N-terminus is retained, which allows binding to extracellular glycosaminoglycans or to other cell surface molecules (Thompson et al., 1994). Because the types of extra-receptor molecules available for EGF family ligands to interact with can vary with spatial location, the spatial range over which autocrine EGF family ligands can spread before binding an EGFR can influence the overall cell receptor binding dynamics and distribution, potentially leading to profound effects on cell responsiveness in vitro and presumably in the intact animal (Cook et al., 1995).

Previous investigations of autocrine signaling loops have encompassed a wide breadth of cellular events including those leading up to ligand-release (Arribas et al., 1996; Dong et al., 1999; Pandiella and Massague, 1991; Peschon et al., 1998), ligand-binding (Lauffenburger et al., 1998), and downstream signaling along with subsequent cell behavior (Dong et al., 1999; Wiley et al., 1998). These studies have focused on endpoint read-outs such as cell and tissue morphology, proliferation, and changes in the state of signaling molecules. However, there is presently little information concerning how cell parameters, such as receptor numbers or ligand expression levels, affect the behavior of autocrine loops. This is important from a practical as well as theoretical standpoint. The great utility of the standard ‘dose-response’ curve used in thousands of studies of biological studies is that it allows predictions of the response of cells to the addition of a given amount of ligand. What is the equivalent paradigm for autocrine loops? How are autocrine loops, in fact, regulated by cells? By alterations in receptor density, ligand production or ligand type? These questions are important, but largely unexplored.

In an effort to better understand autocrine signaling, we investigate here the spatial operation of an autocrine loop by determining the fraction of ligand captured locally by the producing cells. This quantity can indicate the spatial range over which autocrine ligands travel before binding to their cognate cell surface receptor. When this ‘local capture fraction’ is close to unity, the spatial domain of the autocrine loop is in the order of the cell dimension, whereas when it is close to zero the spatial domain of the autocrine loop is many multiples of the cell dimension. In addition, the amount of ligand captured, and thus consumed locally by cells, should reflect the net activity of the autocrine loop.

We demonstrate here that the activity of an autocrine loop can be characterized in terms of the ratio of the ligand production rate to that of receptor production. Embedded in these production rates are two key cell properties, ligand release rate and cell surface receptor number. Our previous modeling efforts have shown that these two properties influence overall quantitative dynamics of autocrine system operation (Forsten and Lauffenburger, 1992; Forsten and Lauffenburger, 1994; Oehrtman et al., 1998) and that the production ratio should dictate the fraction of ligand captured (Will et al., 1995). In this present experimental study, we use two different assay systems. In one, we measure the fraction of ligand escaping capture and, in the other, we directly measure ligand captured locally. The results are consistent with our hypothesis. As the ligand production rate approaches the receptor production rate, the fraction of ligand captured decreases. This suggests that regulatory processes that control ligand and receptor production rates also regulate the overall activity and spatial operation of autocrine systems. Importantly, our findings demonstrate that cell responses to autocrine ligands can be largely governed under conditions in which ligand is efficiently captured and thus not easily detectable in bulk media.

MATERIALS AND METHODS

Cell culture

Parental B82L mouse fibroblasts transfected with human EGFR were a gift from Gordon Gill. A tetracycline-controlled two-plasmid system (Gossen and Bujard, 1992) was used to transfect B82 wild-type cells with a truncated form of the EGF gene, creating an artificial autocrine system. The truncated EGF gene (ctEGF) consists of the cytoplasmic tail, the transmembrane domain, the mature EGF region and the signal sequence. The gene does not contain amino extension after the mature EGF region and before the signal sequence. The ctEGF gene is more fully described elsewhere (Wiley et al., 1998). The cells were grown in Dulbecco’s Modified Eagles Medium (DMEM) with 10% dialyzed calf serum (DCS), penicillin, and streptomycin, all purchased from Gibco. In addition, to maintain selection, we added 1 μM methotrexate (Sigma), 300 μg/ml G418 sulfate (Gibco), 600 Units/ml hygromycin B (Calbiochem), and 2 μg/ml tetracycline (Sigma). Human mammary epithelial cells (HMEC) were obtained and maintained as previously described (Dong et al., 1999).

Modifying ligand secretion rate and cell surface receptor number

Two methods were employed to control the cell’s autocrine ligand production. First, we varied the concentration of tetracycline in the media since tetracycline represses the expression of the gene encoded

in the expression plasmid (Gossen and Bujard, 1992). Second, water-soluble analogs of the metalloproteinase inhibitor batimastat (BB-3103 and BB-2116; obtained from British Biotech, Oxford, UK) were used to decrease the rate of ligand release (Dong et al., 1999).

We controlled the number of available cell surface receptors by adding different concentrations of anti-EGFR monoclonal antibody 225 that blocks EGF binding to the receptor (Gill et al., 1984). Anti-EGFR mAb 225 was obtained and purified from hybridoma obtained from the American Type Culture Collection (Wiley et al., 1998). A concentration of 5 μg/ml mAb was sufficient to completely block the surface receptors (see Fig. 3).

Fractional release of EGF into the medium

Cells were plated in 12-well tissue culture plates in tissue culture media initially at 2×10^5 cells per well. On day 3, we washed the cells twice and added media containing a given concentration of tetracycline and BB-3103. On day 4, we washed the cells once and changed them to media with the same composition as day 3 media, but included only 1% DCS and a variable concentration of mAb 225. After 8-14 hours of conditioning by the cells, we collected the media, centrifuged it at 16,000 ***g*** for 10 minutes, and stored it at –20°C until analysis. Cells in parallel plates were counted to determine the average number of cells per well. We measured the concentration of EGF in the media using an EGF sandwich ELISA, described elsewhere (Wiley et al., 1998; Will et al., 1995) with a standard curve constructed using rhEGF (PeproTech Inc), diluted in base media with 1% DCS. We read the ELISA plate kinetically at 405 nm using a microplate reader.

Microphysiometer assay

Cells were seeded in 12-well transwells on day 1 at 2×10^5 cells per transwell. On the second day, we washed the cells twice with PBS, followed by changing the media to media containing a given concentration of tetracycline and BB-3103. On the third day, we prepared the transwells for placement on the microphysiometer by inserting a spacer. The spacer (6 mm diameter and 50 μm height) partially defines the volume of the cell chamber. Next, we placed a capsule insert with a 3 μm pore membrane into the transwell so that it fit flush. We transferred this assembly into the silicon sensor chambers, and then the chambers were connected to the microphysiometer. Plungers were inserted into the capsule inserts, completing the cell chamber (6 mm diameter and 100 μm height).

The microphysiometer was flushed with media and pre-heated to 37°C before the addition of the completed chambers. The media for the microphysiometer is DMEM without buffer, 2.59 g/l NaCl and 1% DCS. Further additions to the media included tetracycline, BB-3103 and mAb 225, depending on the experiment. The microphysiometer fluid flow was organized with the following pump cycle: pump was 'on' for 43 seconds, flushing the chamber. The pump was 'off' for 27 seconds. During the 'off' cycle, a pause was programmed for the first 5 seconds, then the reading was taken for 20 seconds, and another pause for 2 seconds before the pumps resumed. The total pump cycle was 1 minute and 10 seconds.

The cells on the Cytosensor were equilibrated for 1-2 hours, as indicated by a constant rate of extracellular acidification. After establishing a stable baseline, we added different concentrations of exogenous rhEGF at concentrations ranging from 0.08 to 40 ng/ml. We then recorded the maximum change in the extracellular acidification rate (ECAR) with respect to the baseline. Each transwell was subjected to only one concentration of EGF before being discarded. A similar set-up has been described previously (Lauffenburger et al., 1998).

Values of ECAR were obtained in units of μVolts/second. Each data point was normalized by dividing by the baseline value of ECAR established for a given chamber and multiplying by 100 to give a percent value. The average baseline was calculated from data collected 8-10 minutes prior to the addition of EGF.

Radiolabeled antibody studies

Anti-EGFR monoclonal antibody 13A9 was obtained from Genenetech. Anti-EGFR monoclonal antibody 13A9 was iodinated with ^{125}I (NEN Life Science Products) using Iodobeads (Pierce) according to the manufacturer's recommendations. Free iodine was separated from radio labeled protein using a column (0.8×20 cm) packed with Sephadex G-10.

Cells were plated on 35 mm plates on day 1 (1:10). On day 3, the media was changed to media containing a given concentration of tetracycline and BB-3103. On day 4, the media was changed to HEPES-buffered DMEM, 1% DCS, 0.5 mg/ml bovine serum albumin, and a given concentration of tetracycline and BB-3103. After 4 hours in media, the plates were washed twice with warm saline and 1.5 ml of the media described above was added containing different concentrations of ^{125}I-labeled 13A9. After 3 hours at 37°C, an aliquot of the medium was collected to determine the antibody concentration and the plates were washed four times with ice-cold saline. Surface-associated antibody was determined by acid stripping at 0°C with 50 mM glycine-HCl, 100 mM NaCl, 2 mg/ml polyvinyl pyrrolidone, 2 M urea, pH 3.0. The number of internalized antibodies was determined following cell lysis of the stripped cells with 1M NaOH (Opresko et al., 1995). Parallel plates were counted using a Coulter Counter to determine the average number of cells per well.

Error estimation

For reports of raw data, experimental errors were calculated using standard statistical methods as indicated in the figure legends. Some reported values, however, are derived by calculations and are thus subject to error propagation. For example, if a quantity 'A1' is used together with quantity 'A2' to derive a value of 'B', the error associated with 'B' is calculated as: sqrt $\{[(\partial B/\partial A1)\times(\text{error in A1})]^2 + [(\partial B/\partial A2)\times(\text{error in A2})]^2\}$, where $\partial B/\partial A1$ is the partial derivative of B with respect to A1 and $\partial B/\partial A2$ is the partial derivative of B with respect to A2. Propagated errors are reported as such in the figure legends.

Mammary epithelial cell proliferation

Cells were plated in 12-well tissue culture plates with medium alone, anti-EGFR mAb 225, BB-2116 or EGF. We changed the media every other day. On day 6, the number of cells per well was counted. In parallel, cells were plated in 60 mm tissue culture plates with the same concentrations of BB-2116 as used above and with anti-EGFR mAb 225. After cells conditioned their media for 18 hours, we collected the media. The concentration of TGF-α in the media was determined by RIA (Dempsey and Coffey, 1994). No TGF-α was found to accumulate in the media in the absence of anti-EGFR mAb 225.

RESULTS

Effect of ligand secretion rate on the fraction of captured ligand

Our engineered autocrine system provides two useful ways to control the rate of ligand production: tetracycline regulation of gene expression, and regulation of proteolytic ligand release using metalloprotease inhibitors (such as BB-3103). Because binding of EGF to its receptor in our system absolutely requires its proteolytic release (Dong and Wiley, 2000), blocking release effectively prevents ligand 'production.' Using both tetracycline and BB-3103 in the media, we were able to vary ligand production rates from less than 100 molecules/cell/minute to nearly 4000 molecules/cell/minute. The rate of the ligand production and release into the medium was found to be constant over a period of 12 hours, as shown in Fig. 1. This was the case in both the presence and absence of an

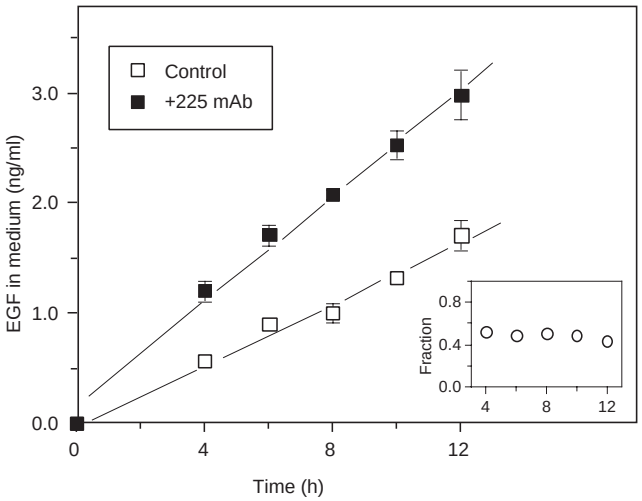

Fig. 1. EGF accumulation in the bulk medium in the presence and absence of EGFR-blocking antibodies. Monolayers of cells were induced to produce EGF at a rate of approximately 1000 molecules×cell^{-1}×min^{-1} using tetracycline. Fresh medium with (■) or without (□) 5.0 μg/ml 225 mAb was added to the cells and, at the indicated time, the medium was collected and assayed for EGF using an ELISA. The fraction of EGF captured, as calculated from the ratio of EGF concentrations without and without 225 mAb, remained constant over 12 hours (insert). The error bars represent the s.d. of one experiment in duplicate.

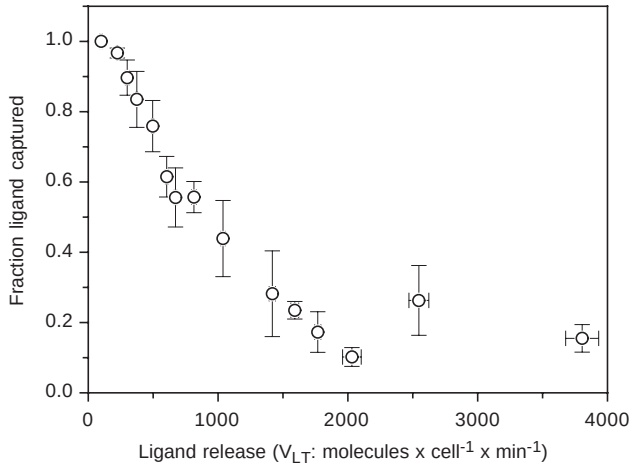

Fig. 2. The fraction of ligand that is captured decreases as ligand release increases. Cells that had been induced to release ligand at different rates using tetracycline and a ligand-release inhibitor were allowed to condition their medium for 8-14 hours. The medium was collected and assayed for EGF by ELISA. The concentration of EGF was then converted to a ligand secretion rate. The total ligand secretion rate, V_{LT}, was calculated from samples containing 5.0 μg/ml 225 mAb during cell medium conditioning. Fraction ligand captured is determined by comparing ligand secretion rates calculated from samples without 5.0 μg/ml 225 mAb to those with 5.0 μg/ml 225 mAb during cell medium conditioning. The error bars represent the s.e.m. of a set of data points taken and analyzed in duplicate.

antagonistic anti-EGFR blocking antibody (mAb 225) sufficient to block uptake of EGF by the cells (5 μg/ml, see Fig. 3).

The amount of ligand found in the medium when all of the receptors are blocked will be proportional to the total ligand production rate. Thus the amount of ligand captured by cells is simply the difference between accumulated ligand observed in the presence and absence of receptor-blocking antibodies. The fraction of captured ligand, f_{LC}, is $1–L_{rem}/L_{tot}$ where L_{rem} is the remaining ligand and L_{tot} is the total ligand for parallel samples. The fraction of captured ligand is essentially constant over the entire 12 hour period of our assay (Fig. 1, insert), indicating that once the ligand enters the bulk medium, it is not lost by secondary processes such as adsorption or extracellular proteolysis.

The accumulation rate of EGF in the medium in the presence of mAb 225 was converted to a rate of ligand production, V_{LT}, by considering the number of cells, volume of medium, and incubation time. After varying the rate of ligand production with tetracycline and BB-3103, as outlined above, we determined the relationship between V_{LT} and f_{LC}. As shown in Fig. 2, the fraction of ligand captured by the cells decreased as the ligand production rate increased. As the ligand secretion rate becomes very large, the fraction of ligand captured appeared to asymptotically approach zero, due to saturation of the EGFR (Will et al., 1995). Thus, our experimental system allows us to explore ligand production rates across a spectrum of the cells' capacity to use that ligand.

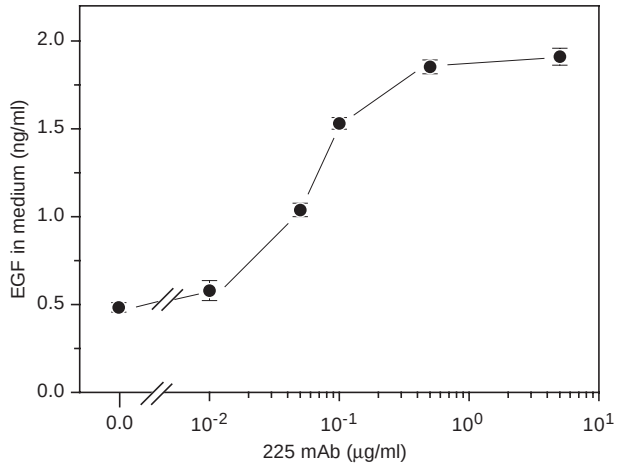

Fig. 3. As the concentration of anti-EGFR blocking antibody increases, the concentration of EGF in the bulk medium increases. Cells induced to secrete ligand at a rate of approximately 600 molecules×cell^{-1}×minute^{-1} using tetracycline were allowed to condition their medium in the presence of 0.0, 0.05, 0.1, 0.5 or 5.0 μg/ml 225 mAb for 12 hours. The medium was collected and assayed for EGF by ELISA. The error bars represent the s.d. of one experiment in duplicate.

Effect of cell surface receptor number on ligand capture

The ability of cells to bind and use autocrine ligands is necessarily dictated by the expression level of the cognate receptor. To determine the relationship between receptor expression and fraction of captured ligand, we varied cell surface receptor number by using different concentrations of mAb 225. As might be expected, increasing the amount of blocking antibody caused an increase in the amount of ligand

found in the extracellular medium (Fig. 3). To convert the concentration of blocking antibody to a number of accessible surface receptors, we used the kinetic model described in Appendix A. We considered both the rate at which the antibody bound to the receptor and the rate at which it dissociated. We also accounted for the rate at which the antibody-receptor complex was internalized and recycled, as well as the rate at which receptors were replenished by synthesis and recycling. The parameter values used in our calculations were either directly measured for this study (such as k_{on} and k_{off} rate constants for antibody-receptor binding), or have been previously published by our laboratories. The number of potentially accessible receptors was calculated as the total number of surface receptors minus the number of antibody-bound surface receptors. The assumptions on which these calculations were based (such as an absence of antibody-induced receptor degradation) were directly tested by independent experiments (results not shown).

We converted the concentration of mAb 225 into the number of surface receptors potentially available for autocrine ligand binding. We then measured the relationship between the number of potential receptors and the actual fraction of ligand captured using cells producing ligand at rates ranging between 90 to 1700 molecules per cell per minute (Fig. 4A). As might have been expected, the higher the number of receptors, the higher the fraction of captured ligand. The higher the ligand production rate, the higher the number of receptors required to capture ligand.

The relationship between receptor levels, ligand production and fractional ligand capture appeared to be complicated. However, a careful examination of the data indicated that ligand capture was efficient only when ligand production was less than receptor production. To clarify this relationship, we converted receptor numbers to the rate of receptor production as described in Appendix A. The ratio of ligand production to receptor production (V_{LT}/V_R) was calculated for each data point shown in Fig. 4A and plotted against the fraction of ligand captured. As shown in Fig. 4B, all of the data collapsed to a single curve. The data from Fig. 2 was also converted to the fraction of ligand captured as a function of V_{LT}/V_R ratio and this also fell on the same curve (Fig. 4B). It appears that for V_{LT}/V_R ratios of <0.2, EGF capture is very efficient and thus spatially localized. As the ratio exceeds 1, the system appears to saturate and most of the ligand appeared in the medium.

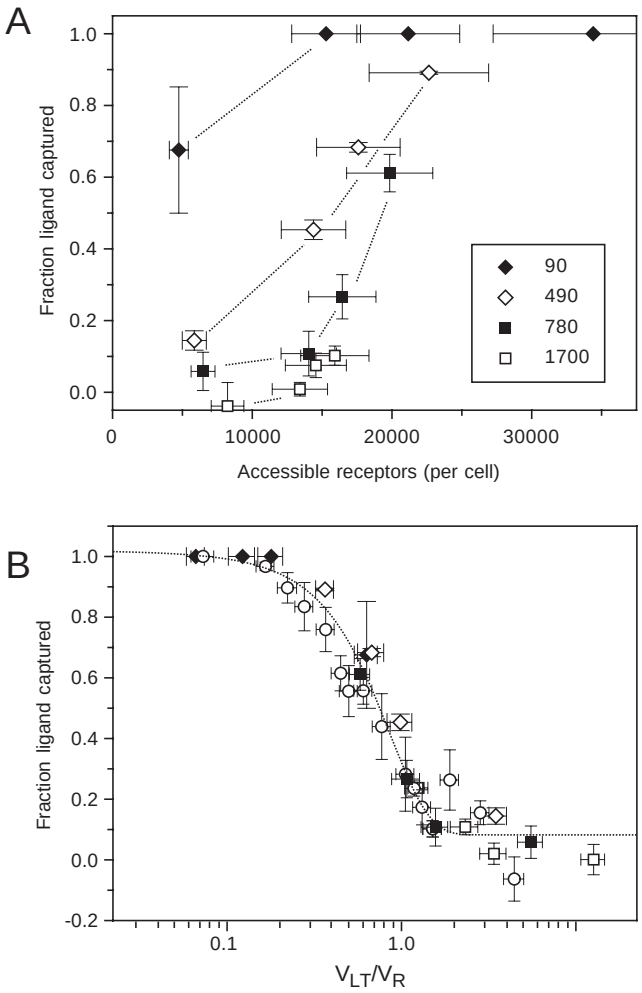

Fig. 4. The relationship between EGF production, EGFR expression and fraction of EGF captured. (A) Cells were induced to release ligand at the rate of 90 (◆), 490 (◇), 780 (■) and 1700 (□) molecules×cell^{-1}×minute^{-1} using tetracycline and a ligand-release inhibitor. Fresh medium with 0.0, 0.05, 0.1, 0.5 and 5.0 μg/ml 225 mAb was then added, and the cells were allowed to condition their medium for 8-14 hours. The medium was collected and assayed for EGF by ELISA. Fraction ligand captured was calculated as described in Fig. 2. The concentration of 225 mAb was converted to number of accessible surface receptors as described in Appendix A. The y error bars represent the s.e.m. of a set of data points taken and analyzed in duplicate. The x error bars represent propagated error as described in Materials and Methods. (B) The data presented in Figs 2 (○) and 4A were used to calculate the effective receptor production rate in molecules×cell^{-1}×minute^{-1} (V_R) at a certain total ligand secretion rate (V_{LT}) for a given concentration of 225 mAb as outlined in Appendix A. The error bars represent propagated error as described in Materials and Methods. The line through the data is a Gaussian distribution fit by least squares and weighed by the estimated errors.

Ligand production rates and receptor activation

The above data indicates that cells can very effectively capture ligand up to the point where the V_{LT}/V_R ratio is ~0.3. However, the relationship between capture efficiency and receptor occupancy is unknown. Occupancy cannot be directly determined by competition assays using radioactive tracer ligands because these assays only measure loss of binding sites. Receptors can be 'lost' by physical removal as well as by occupancy. Thus the results of these assays are always ambiguous. To directly measure the degree of receptor activation and thus occupancy, we used a Molecular Devices cytosensor.

A cytosensor measures the rate at which cells acidify their environment (extracellular acidification rate: ECAR) and is widely used for monitoring receptor-mediated responses of cells to exogenous ligands (McConnell et al., 1992). We have also recently demonstrated that it can be used for quantifying cell responses to autocrine ligands (Lauffenburger et al., 1998). We thus used this device to determine the fraction of receptors occupied at a given level of autocrine ligand production.

The addition of EGF induced an increase in the ECAR value of B82 cells (Fig. 5A). The shape of the response curve was essentially independent of ligand concentration. Therefore, we used the peak normalized ECAR value as an indicator of

receptor activation. This value, referred to as ECAR-Max, was found to be proportional to the concentration of added EGF and was thus proportional to receptor occupancy (Lauffenburger et al., 1998).

The relationship between ECAR-Max and EGF concentration described a smooth curve (Fig. 5B). In the case of cells producing autocrine EGF, the curve was shifted downward, and the greater the level of endogenous EGF production, the greater the shift in the curve (Fig. 5B). We have previously suggested that this effect is due to an increase in the ECAR baseline caused by autocrine ligand binding (Lauffenburger et al., 1998). Subtracting this higher baseline during the data normalization process results in the downshifted curve. Potentially, the degree of the shift indicates the number of endogenous ligand-receptor complexes.

To quantify this effect, we assumed that to generate the same response above the baseline (i.e. the same value of ECAR-Max), required a constant number of newly formed receptor-ligand complexes under any given condition. We thus calculated the number of newly formed complexes using a kinetic model outlined in Appendix B. An important input for this determination of newly formed complexes is the number of free surface receptors available just before the addition of exogenous ligand (i.e. the baseline), which is governed by steady state autocrine ligand binding. Since the number of newly formed complexes thereby depends on the level of autocrine ligand, we calculated the effective autocrine ligand concentration by requiring it to fulfill the criterion that a given ECAR-Max demands a constant number of newly formed complexes. As shown in Fig. 6, the calculated effective autocrine ligand concentration ($[L]_{A,eff}$) was directly proportional to the ligand production rate. This indicates that the downward shift in the ECAR curves shown in Fig. 5B is directly correlated with the level of autocrine ligand production. From $[L]_{A,eff}$, we calculated the number of receptor-ligand complexes created by autocrine ligand capture, and thus the fraction of cell receptors occupied by ligand.

We calculated both the fraction of surface receptors occupied by autocrine ligand as well as the fraction of total cell receptors (surface plus internalized receptors). These values were then plotted against the ratio of ligand and receptor production (V_{LT}/V_R ratio). As shown in Fig. 7, the fraction of occupied receptors was proportional to the V_{LT}/V_R ratio. The occupied fraction of total receptors was higher than surface receptors, because occupancy-induced receptor internalization allowed accumulation of occupied receptors inside the cells. For comparison, the curve describing the fraction of ligand that was captured is included in Fig. 7. It can be seen that when ligand capture is >90%, receptor occupancy is 30-40% and the V_{LT}/V_R ratio is approximately 0.3. At levels of ligand production sufficient to occupy >90% of the receptors, ligand capture drops to <10% and the V_{LT}/V_R ratio rises to >1. Thus a significant amount of autocrine signaling occurs when there is little detectable ligand in the extracellular medium. High levels of receptor occupancy, however, require a great excess of ligand production over receptor production.

Autocrine signaling in mammary epithelial cells

The relationship between V_{LT}/V_R ratios and cell responses was defined above using artificial autocrine systems. To understand how these finding might apply to natural autocrine cells, we examined the relationship between TGF-α production and cellular responses in human mammary epithelial cells (HMEC). These cells are dependent on autocrine signaling through the EGFR for proliferation in culture (Wiley et al., 1998). As shown in Fig. 8A, blocking the EGFR by the addition of mAb 225 inhibited proliferation of HMEC by

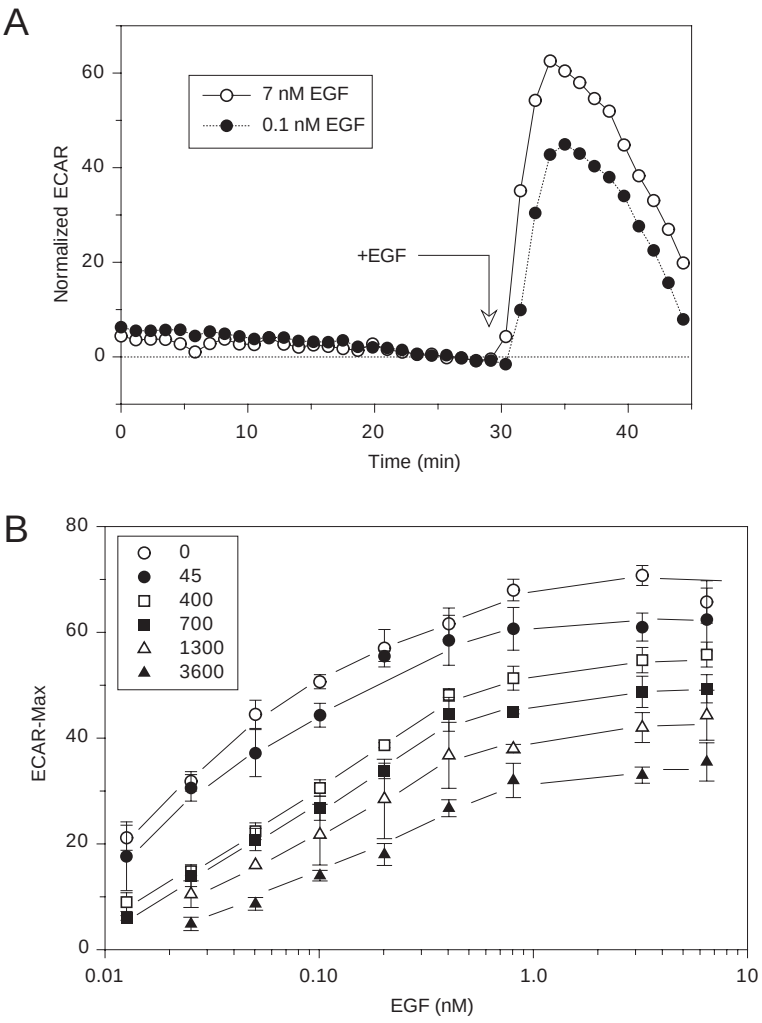

Fig. 5. ECAR increases in response to increasing endogenous and exogenous EGF. (A) Cells lacking EGF expression were grown in transwells and placed in a cytosensor. Once a baseline ECAR was established, the cells were challenged with an addition of exogenous EGF, 7 nM (○) or 0.1 nM (●). The reported ECAR is normalized to the baseline signal that was set to 0 for clarity. (B) Cells were induced to secrete ligand at a steady state rate of 0 (○), 45 (●), 400 (□), 700 (■), 1300 (△), 3600 (▲) molecules×cell^{-1}×minute^{-1} using tetracycline and a ligand-release inhibitor. The cells were placed on the cytosensor and once a baseline was established, they were challenged with 40, 20, 5, 2.5, 1.2, 0.6, 0.3, 0.15, 0.08 ng/ml EGF. The maximal change in ECAR, normalized to baseline, was recorded as a function of the challenge concentration. The error bars represent the s.e.m. of three experiments in duplicate.

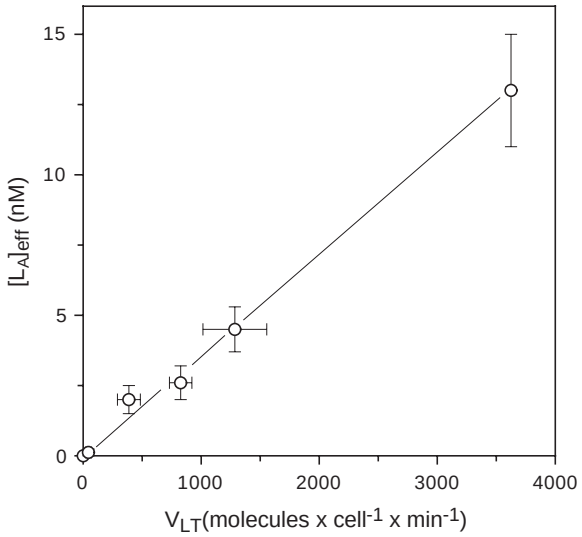

Fig. 6. The effective autocrine ligand concentration increases as ligand secretion increases. The effective autocrine ligand concentration was calculated by using the cytosensor data shown in Fig. 5B in conjunction with the whole cell model outlined in Appendix B. The error bars represent propagated error propagated from the s.e.m. of receptor synthesis rate, the s.e.m. of the fraction of ligand degraded, the s.e.m. of the ligand production rate, and the standard error of the estimate associated with the ECAR-Max curve fits.

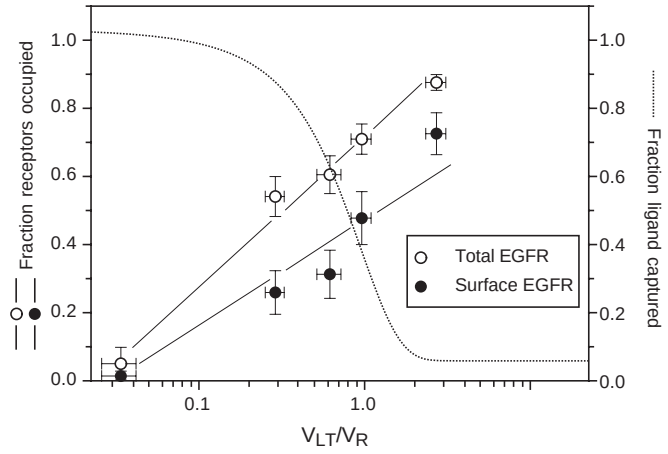

Fig. 7. Fraction of occupied receptors increases as ligand secretion increases. The fraction of occupied receptors was calculated by using the cytosensor data shown in Fig. 6 with the whole cell model outlined in Appendix B and can be calculated based on the total number of occupied receptors (○) or the number of occupied surface receptors (●). The error bars represent propagated error from the s.e.m. of receptor synthesis rate, the s.e.m. of the fraction of ligand degraded, the s.e.m. of the ligand production rate, and the standard error of the estimate associated with the ECAR-Max curve fits. The dashed line (⋯) represents the data from Fig. 4B.

approximately 80%. A similar degree of inhibition was obtained by blocking surface metalloprotease activity. The addition of high concentrations of exogenous EGF, however, induced a threefold increase in cell number over control values. Thus, endogenous autocrine signaling through the EGFR produces approximately 20-30% of the maximal response.

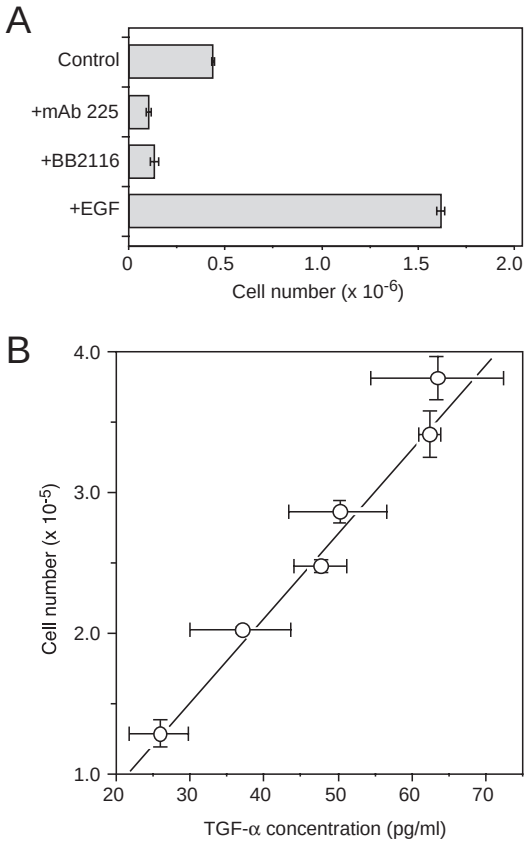

Fig. 8. Autocrine signaling in human mammary epithelial cells. (A) Cells were grown in 12-well dishes for 6 days with medium alone (control), mAb 225 (10 μg/ml), BB-2116 (10 μM) or EGF (2 nM). The medium was changed every other day and the cells were counted on day 6. (B) Cells were grown as described above with concentrations of BB-2116 ranging from 0.01 to 10 μM. Cell numbers were determined on day 6. Parallel cultures of cells in 60 mm dishes were treated with the same concentrations of BB-2116 and 20 μg/ml of mAb 225 for 18 hours. The medium was then collected and the TGF-α levels were determined by RIA. Cell number was 2×10^6 per dish. Error bars represent the SD of triplicate samples.

TGF-α appears to be the most important EGFR ligand and its proteolytic release appears to be required for its activity (Dong et al., 1999). We therefore inhibited the release of TGF-α by adding different concentrations of the metalloprotease inhibitor BB2116 and measured HMEC proliferation. In parallel, release of TGF-α was evaluated in the presence of a saturating amount of mAb 225 (20 μg/ml) to prevent uptake by cells. As shown in Fig. 8B, HMEC proliferation was directly proportional to the amount of released TGF-α. The maximal rate of release (64 pg/ml in 18 hours) was converted to V_{LT}, yielding a value of 15 molecules/cell/minute. We have previously shown that the value of V_R for HMEC is $2\text{-}4\times10^4$ molecules/cell/minute (Burke and Wiley, 1999). Thus the V_{LT}/V_R ratio for autocrine signaling through the TGF-α/EGFR pair in HMEC is approximately 5×10^{-4}. This suggests that in the case of TGF-α autocrine signaling through the EGFR, receptor production is in vast excess over ligand production. This indicates that ligand production is the proximal regulator of EGFR activity in HMEC.

DISCUSSION

Autocrine systems are generally difficult to study because they are self-contained, recursive systems. To understand their operation, one must be able to experimentally vary functionally important system parameters and to measure the consequent cellular responses. Our approach was to engineer an artificial autocrine system in which we could vary both receptor level and ligand production rate. The effect of varying these two parameters was determined by measuring several different responses in an effort to define the general features of autocrine systems. We were particularly interested in the following issues: what is the best way to define the activity of an autocrine system? What is the relationship between ligand production and receptor occupancy? Can we quantitatively define the activity of an autocrine system by sampling the extracellular medium?

Experimentally, we are limited by what we can reliably measure in our system. This includes the rate of ligand accumulation in the medium, the number of empty receptors, the response of the cells to a challenge with exogenous ligand and the distribution of anti-receptor antibody 'tags' between different cellular compartments. Using these and other directly measured parameters (such as binding rate constants), we were able to reliably estimate the value of other cellular parameters, such as the degree of receptor occupancy. We validated our estimates by showing excellent agreement between predicted and experimentally determined values for receptor distribution, receptor numbers and effective ligand concentrations (see Appendix B). The assays used for our primary data measurements are robust (i.e. ELISA assays and cytosensor measurements). Furthermore, the data collected over an extended period could be readily plotted on a single curve (see Fig. 4B). Thus, we are confident that our methodology provides a reasonable basis for understanding the operation of autocrine systems.

We found that although the relationship between ligand production, receptor number and ligand capture appeared complicated, it could be greatly simplified by using the ratio of ligand production to receptor production as the defining system parameter. On the face of it, this simplification makes sense. If ligand is produced faster than receptors, then the system will obviously become saturated. The V_{LT}/V_R ratio, in effect, specifies the 'dose' of an autocrine ligand relative to receptor levels. To demonstrate the usefulness of the V_{LT}/V_R ratio as an experimental parameter, we varied the value of V_{LT} by using either inhibitors or changing the level of ligand expression. In addition, we varied V_R by the addition of receptor-blocking antibodies. Regardless of the method used to vary the V_{LT}/V_R ratio, we found a constant relationship between the ratio and relevant system parameters, such as the fraction of ligand that was captured. Thus, the V_{LT}/V_R ratio is a useful indicator of the activity of an autocrine system. Note that we use the term V_R instead of receptor number so that the ratio will be dimensionless. V_R is simply the rate of receptor 'production' or appearance at the cell surface and can be estimated as the product of surface receptor number and its constitutive internalization rate (usually 0.03 minute^{-1}; see Appendix A).

By using the V_{LT}/V_R ratio as a system parameter, we can define three regimes characteristic of autocrine EGFR signaling. At a V_{LT}/V_R ratio of <0.2, essentially no ligand appears in the medium, but up to 20% of the receptors are occupied. In this regime, signaling is 'invisible' in that sampling the extracellular medium will not reveal the presence of the autocrine ligand. For example, we could not detect TGF-α in the extracellular medium of HMEC unless we first blocked their EGFR. By direct measurement, we found that the V_{LT}/V_R ratio of the TGF-α/EGFR pair in HMEC was approximately 5×10^{-4} (Fig. 8). Although this is a surprisingly low value, similar values can be calculated from the observed production rate of TGF-α in other autocrine systems (Valverius et al., 1989). HMEC produce other EGFR ligands, such as amphiregulin, but we have found that their rate of production could only raise the V_{LT}/V_R ratio to approximately 1×10^{-2} (data not shown). Interestingly, HMEC display a relatively high value of V_R because of rapid recycling of the EGFR (Burke and Wiley, 1999). This process lowers the V_{LT}/V_R ratio about tenfold. Nevertheless, we found that in HMEC, cellular responses were directly proportional to the V_{LT}/V_R ratio. The low V_{LT}/V_R ratio regime appears to be characteristic of many cell types that depend on the EGFR system for growth and proliferation, including many transformed cells (Dempsey and Coffey, 1994; Dong et al., 1999; Van de Vijver et al., 1991). This suggests that EGFR production is normally in vast excess over ligand production and that cellular responses are regulated primarily through ligand availability and capture.

At a V_{LT}/V_R ratio of between 0.2 and 1.0, we found that the EGFR system became progressively saturated and significant amounts of ligand appear in the medium. This is visible autocrine signaling and is apparent in EGFR systems when ligand production is enhanced by pharmacological agents, such as phorbol esters (Kudlow and Bjorge, 1990). The loss of autocrine ligands into the medium may also be facilitated by the reduction in EGFR affinity that is characteristically produced by agents such as phorbol esters (Lund et al., 1990). Above a V_{LT}/V_R ratio of 1.0, the receptor system is saturated and most ligand appears in the extracellular medium. We are unaware of any natural autocrine system in which the receptor system is saturated.

Although we have used the EGF-EGFR autocrine system as our model, most of our findings should be directly applicable to other autocrine systems. For example, a V_{LT}/V_R ratio of >1 should generally result in saturation. However, the quantitative relationship between V_{LT}/V_R ratios and cellular responses will be system specific. Models we have previously developed indicate that receptor density and binding affinity are important cellular properties modulating the operation of autocrine systems (Forsten and Lauffenburger, 1992; Forsten and Lauffenburger, 1994; Oehrtman et al., 1998). There are also differences between steady state and transient autocrine signaling. For example, both the ELISA-based fractional capture assay and the cytosensor assay show qualitative similar results. However, at a V_{LT}/V_R ratio where the ELISA assays shows a f_{LC} equal to near unity, calculations using the cytosensor data indicates a f_{LC} equal to approximately 0.4. Our interpretation is that these two experimental systems investigate different points between two extremes: the fraction of ligand captured at steady state and the fraction captured on the 'first-pass'.

The issues of ligand capture at steady state and on first-pass have been addressed theoretically in earlier work (Berg and

Purcell, 1977; Forsten and Lauffenburger, 1994). Berg and Purcell analyzed steady state transport of a ligand outside a cell's microenvironment to the cell surface and predicted the probability of ligand capture as a function of receptor density (Berg and Purcell, 1977). More recently, a Brownian dynamics simulation (BDS) computation has been used to predict the first-pass capture as a function of receptor density (Forsten and Lauffenburger, 1994). The steady state and first-pass analyses predict markedly different ligand capture probabilities at intermediate receptor numbers. Above 300,000 receptors per cell, both models approach a unity probability of capture. Below 10,000 receptors per cell, both models approach zero. The steady state analysis predicts higher probabilities of ligand capture for intermediate receptor densities and low ligand secretion rates (Forsten and Lauffenburger, 1994). At the receptor level displayed by our cells (~45,000 per cell) steady state analysis predicts a probability of capture of 0.8, whereas the BDS predicts 0.2. This is in reasonable agreement with the values obtained from our ELISA versus the cytosensor measurements. The very low V_{LT}/V_R ratio that we observed in HMEC suggests that TGF-α capture at the cell surface is normally very efficient.

We have shown that the activity of an autocrine system can be defined in terms of the V_{LT}/V_R ratio. This ratio is controlled by cellular properties such as ligand expression levels, surface protease activity and number of cell surface receptors. Although we have manipulated these properties artificially, numerous experimental studies have shown that cells can actively regulate these parameters. For example, ligand expression is under feedback control (Kudlow and Bjorge, 1990). The activity of metalloproteases that regulate EGFR ligand release is also acutely regulated by protein kinase C activity (Dong and Wiley, 2000; Pandiella and Massague, 1991), Ca^{2+} release (Dong and Wiley, 2000; Pandiella and Massague, 1991), cell adhesion and spreading (Gechtman et al., 1999), and MAPK activation (Gechtman et al., 1999). The number of cell surface receptors displayed by a cell can be altered by downregulation through recycling (Herbst et al., 1994; Wiley et al., 1991), receptor synthesis (Eisenkraft et al., 1991) and constitutive internalization (Burke and Wiley, 1999). The experimental and computational approaches outlined here should prove useful in understanding how alterations in these parameters affect the response of cells to autocrine signaling.

An especially interesting and important application may be to breast and related cancers, concerning how changes in these cell-level parameters may be involved in malignant cell transformation. For example, overexpression of autocrine TGF-α has been found to be associated with hyperplasia in mammary epithelium but not necessarily in other tissues (Matsui et al., 1990), and fibroblast transformation has been found to vary with expression levels of both TGF-α and EGFR (Dimarco et al., 1989). Analysis of such outcomes in terms of the kinds of fundamental quantitative principles we have begun to elucidate may help deconvolute some aspects of pathophysiology signaling complexity.

APPENDIX A

The calculation of the number of ligand-assessable receptors and the effective receptor appearance rate, based on the concentration of blocking antibody used in an experiment, requires solving a set of six equations describing receptor-ligand and receptor-antibody binding and trafficking at steady state. The assumptions embedded in these calculations are that the concentration of antibody and the concentration of endogenous ligand do not change during the time course of the experiment and that the antibody remains bound to receptor upon recycling.

The descriptions of each of the six equations are as follows. Eqn AA1 describes the time rate of change of free surface receptors; Eqn AA2 describes the time rate of change of receptor-ligand surface complexes; Eqn AA3 describes the time rate of change of receptor-ligand internal complexes; Eqn AA4 describes the time rate of change of total internal receptors; Eqn AA5 describes the time rate of change receptor-antibody surface complexes; and Eqn AA6 describes the time rate of change of receptor-antibody internal complexes.

$$\frac{dRs}{dt} = -kf * Rs * L_{endo} + kr * Cs_{endo} - k_{eR} * Rs + k_{rec} * (1 - fR) * RiT + V_S - 2k_{on} * B * Rs + k_{off} * Ys \quad \text{(AA1)}$$

$$\frac{dCs_{endo}}{dt} = kf * Rs * L_{endo} - kr * Cs_{endo} - k_{eC} * Cs_{endo} \quad \text{(AA2)}$$

$$\frac{dCi_{endo}}{dt} = k_{eC} * C_{endo} - [k_{rec} * (1 - fR) + k_{dgr} * fR] * Ci_{endo} \quad \text{(AA3)}$$

$$\frac{dRiT}{dt} = k_{eR} * Rs + k_{eC} * Cs_{endo} - [k_{rec} * (1 - fR) + k_{dgr} * fR] * RiT \quad \text{(AA4)}$$

$$\frac{dYs}{dt} = 2 * k_{on} * B * Rs - k_{off} * Ys - k_{eY} * Ys + k_{rec} * (1 - fR) * Yi \quad \text{(AA5)}$$

$$\frac{dYi}{dt} = k_{eY} * Ys - [k_{rec} * (1 - fR) + k_{dgr} * fR] * Yi \quad \text{(AA6)}$$

For different blocking antibody concentrations, the steady state number of ligand-accessible surface receptors is calculated from the solutions of Eqns AA1-AA6 as the total number of surface receptors minus those surface receptors bound by blocking antibody.

The appearance rate of surface receptors, V_R, is equal to the rate of receptor synthesis plus the rate of receptor recycling to the surface at steady state in the absence of ligand. Solving Eqn AA1 at steady state also shows that V_R is also equal to the constitutive internalization rate multiplied by the number of surface receptors in the absence of ligand (Eqn AA8).

$$V_R = V_s + k_{rec} * (1 - fR) * RiT_o = k_{eR} * Rs_o \quad \text{(AA7)}$$

For different blocking antibody concentrations, the steady state number of ligand-accessible surface receptors is calculated as described above. Then V_R is calculated using this number for a given blocking antibody concentration as Rs_o in Eqn AA7.

The values of the rate constants used in the above equations

Table A1. Rate constants

Variable	Definition	Refs
B	Concentration of mAb 225 in M	
L_{endo}	Concentration of endogenous ligand in M	
k_{on} = 2*10^7 M^{-1} min^{-1}	Association rate constant for R/Ab	A.E.D. et al., unpublished
k_{off} =0.02 min^{-1}	Dissociation rate constant for R/Ab	A.E.D. et al., unpublished
k_{eY} = 0.07 min^{-1}	Internalization rate constant of R/Ab	A.E.D. et al., unpublished
kf = 6.3 *10^7 M^{-1} min^{-1}	Association rate constant for R/L	French et al., 1995
kr = 0.16 min^{-1}	Dissociation rate constant for R/L	French et al., 1995
k_{eC} = f (Cs)	Internalization rate constant	Lund et al., 1990
k_{eR} = 0.03 min^{-1}	Constitutive internalization rate constant	Wiley et al., 1991
V_S = 300 molecules $cell^{-1}$ min^{-1}	Synthesis rate of receptor	A.E.D. et al., unpublished
fR = 0.45	Fraction of internal receptors degraded	French et al., 1995; Herbst et al., 1994; French et al., 1994
k_{dgr} = 0.022 min^{-1}	Degradation rate constant	French et al., 1995; French et al., 1994
k_{rec} = 0.058 min^{-1}	Recycling rate constant	Herbst et al., 1994

are described and listed in Table A1. The receptor synthesis rate, V_S, was calculated using Eqn AA8 that represents a steady state sorting condition of receptors in the absence of ligand. The number of surface receptors at steady state, Rs_o, was determined using a non-blocking, radiolabeled anti-EGFR antibody as a tag (mAb 13A9).

$$V_S = \frac{Rs_o * k_{eR}}{1 + \frac{k_{rec} * (1 - fR)}{k_{dgr} * fR}} \quad \text{(AA8)}$$

APPENDIX B

The calculation of the fraction of occupied surface receptors from the ECAR-Max data requires the solutions to two sets of equations. One set of equations is solved at steady state and the other transiently. The assumptions embedded in these equations are that the concentrations of exogenous ligand and endogenous ligand do not change during the time of the experiment and the observed differences in the microphysiometer responses for different V_{LT} values are solely due to a difference in the number of receptors available for exogenous ligand binding. Receptor de-sensitization due to endogenous ligand does not appear to play a significant role in the ECAR-Max differences observed for different V_{LT} values, as indicated by Fig. 9. This figure shows that for the same available free surface receptors, whether the unavailable receptors are bound by ligand or blocking antibody, ECAR-Max as a function of added ligand was the same. The values for rate constants in Eqns AB1-6 are the same as values listed in Appendix A.

The following four equations are solved at steady state and describe receptor-ligand binding and trafficking. The solution to these equations is used to determine the number of surface receptors available for exogenous ligand binding as a function of the concentration of endogenous ligand. Eqns AB1 and AB3 describe the time rate of change of the number of endogenous complexes on the surface and inside the cell, respectively. Eqns AB2 and AB4 describe the time rate of change of free surface receptors and total internal receptors, respectively.

$$\frac{dCs_{endo}}{dt} = kf * Rs * L_{endo} - kr * Cs_{endo} - k_{eC} * Cs_{endo} \quad \text{(AB1)}$$

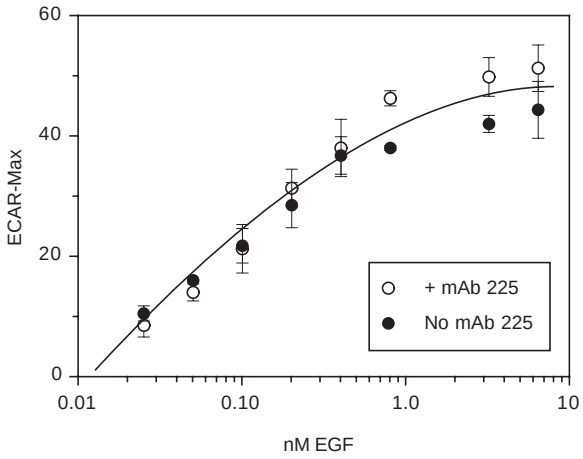

Fig. 9. Receptor de-sensitization is not responsible for the shift in ECAR-Max as cells release more ligand. Cells releasing ligand at 1300 (○) and 830 (●) molecules×$cell^{-1}$×$minute^{-1}$ as controlled by tetracycline concentration and a ligand-release inhibitor were placed on the cytosensor with (○) or without (●) 0.1 μg/ml 225 mAb in the medium. This resulted in both cells with essentially the same number of surface accessible receptors (7500 per cell). The cells were challenged with 40, 20, 5, 2.5, 1.2, 0.6, 0.3, 0.15 ng/ml EGF and the ECAR-Max was determined as described in Fig. 5. The error bars represent the s.e.m. of three experiments in duplicate.

$$\frac{dRs}{dt} = -kf * Rs * L_{endo} + kr * Cs_{endo} - k_{eR} * Rs + k_{rec} * (1 - fR) * RiT + V_S \quad \text{(AB2)}$$

$$\frac{dCi_{endo}}{dt} = k_{eC} * Cs_{endo} - [k_{rec} * (1 - fR) + k_{dgr} * fR] * Ci_{endo} \quad \text{(AB3)}$$

$$\frac{dRiT}{dt} = k_{eR} * Rs + k_{eC} * Cs_{endo} - [k_{rec} * (1 - fR) + k_{dgr} * fR] * RiT \quad \text{(AB4)}$$

The following two equations are solved transiently and describe the formation of newly formed complexes on the surface (AB5) and inside the cells (AB6) as a result of exogenous ligand addition, essentially describing a challenge of exogenous EGF using the microphysiometer. Recycling and degradation are not included in these two equations because the solutions are

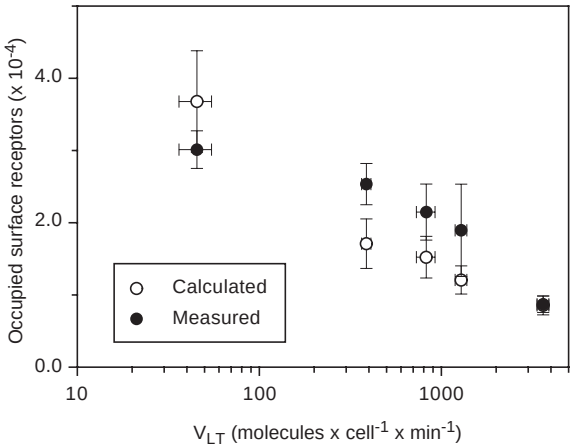

Fig. 10. Whole-cell modeling, with endogenous ligand concentration determined from microphysiometer experiments, predicts the occupancy of surface receptors on autocrine cells. Nearly confluent monolayers of autocrine cells secreting different levels of ligand as controlled by tetracycline and a ligand-release inhibitor were incubated with 0.6 μg/ml ^{125}I-13A9 mAb, an EGFR non-blocking antibody, for 3 hours at 37°C. ^{125}I-13A9 mAb was removed by acid stripping as described in Materials and Methods to determine the number of surface receptors (●). Using whole-cell kinetic modeling as described in Appendix B, the predicted total number of surface receptors was determined (○). The error bars for the radiolabeling results represent the s.e.m. of two to five experiments in triplicate. The error bars for the modeling results represent propagated error from the s.e.m. of receptor synthesis rate, the s.e.m. of the fraction of ligand degraded, the s.e.m. of the ligand production rate, and the standard error of the estimate associated with the ECAR-Max curve fits.

used in a time frame (~5 minutes) that is less than that required for recycling or degradation processes to play a significant role.

$$\frac{dCs_{\text{exo}}}{dt} = kf * (RsT_{\text{exo}} - Cs_{\text{exo}}) * L_{\text{exo}} - kr * Cs_{\text{exo}} - k_{\text{eC}} * Cs_{\text{exo}} \quad \text{(AB5)}$$

$$\frac{dCi_{\text{exo}}}{dt} = k_{\text{eC}} * Cs_{\text{exo}} \quad \text{(AB6)}$$

The total receptors available for exogenous ligand, RsT_{exo}, are the total receptors on the surface minus those receptors complexed with endogenous ligand at steady state. Essentially, this places the solutions for Eqns AB1-4 into the transient solutions for AB5 and AB6, thereby eliminating RsT_{exo} and replacing it with a function of L_{endo}. For different values of V_{LT}, the number of newly formed complexes is equated to the number of newly formed complexes when V_{LT} equals zero for a given microphysiometer response (ECAR-Max), resulting in one equation with one unknown. On one side of the equation is the total number of newly formed complexes when V_{LT} is zero, and on the second side of the equation is the total number of newly formed complexes when V_{LT} is nonzero. This second side contains an unknown, L_{endo}, for which the equation is now solved. L_{endo} is then used to calculate to determine the fraction of receptors occupied ($f_{\text{R occupied}}$) by endogenous ligand via the solutions to Eqns AB1-4. L_{endo} and $f_{\text{R occupied}}$, as calculated using the microphysiometer data, are plotted against values of V_{LT}, measured independently in parallel wells. The relationship between V_{LT} and L_{endo} is now a known function that is used, for example, in Appendix A to calculate available surface receptors for values of V_{LT} other than those measured by the microphysiometer.

Experiments using a tag antibody are conducted to determine how well the steady state models in Appendices A and B describe the level of receptors on the surface of the cells as a function of the level of ligand production. We added a saturating amount of a non-blocking, radiolabeled labeled EGFR antibody (mAb 13A9) to cells secreting different levels of ligand as controlled by tetracycline and a ligand-release inhibitor. The cells were incubated at 37°C for 3 hours. Then we stripped the cell surface using an acid wash and measured the counts associated with the surface. We determined the number of surface receptors at steady state from these counts. We compared these results with the number of cell surface receptors at steady state predicted using our model described above. The results shown in Fig. 10 indicate that the model accurately describes ligand-regulated alterations in surface receptor numbers.

We thank Birgit Will for construction of the autocrine cell system, Margaret Woolf for laboratory expertise and Tomoko Iida for assistance in the laboratory. We also thank Peter Dempsey for performing the TGF-α radioimmunoassays. This work has been supported by a grant from the NSF Bioengineering & Environmental Systems Program to D.A.L. and H.S.W., NIH Grant P01-HD288528, and an NIH Biotechnology Training Grant to A.E.D.

REFERENCES

Arribas, J., Coodly, L., Vollmer, P., Kishimoto, T. K., RoseJohn, S. and Massague, J. (1996). Diverse cell surface protein ectodomains are shed by a system sensitive to metalloprotease inhibitors. *J. Biol. Chem.* **271**, 11376-11382.

Barnard, J. A., Graves-Deal, R., Pittelkow, M. R., DuBois, R., Cook, P., Ramsey, G. W., Bishop, P. R., Damstrup, L. and Coffey, R. J. (1994). Auto- and cross-induction within the mammalian epidermal growth factor-related peptide family. *J. Biol. Chem.* **269**, 22817-22822.

Berg, H. C. and Purcell, E. M. (1977). Physics of chemoreception. *Biophys. J.* **20**, 193-219.

Bier, E. (1998). Localized activation of RTK/MAPK pathways during Drosophila development. *Bioessays* **20**, 189-194.

Bissell, D. M., Wang, S. S., Jarnagin, W. R. and Roll, F. J. (1995). Cell-specific expression of transforming growth-factor-beta in rat-liver – evidence for autocrine regulation of hepatocyte proliferation. *J. Clin. Invest.* **96**, 447-455.

Boussiotis, V. A., Nadler, L. M., Strominger, J. L. and Goldfeld, A. E. (1994). Tumor-necrosis-factor-alpha is an autocrine growth-factor for normal human B-cells. *Proc. Natl. Acad. Sci. USA* **91**, 7007-7011.

Burke, P. M. and Wiley, H. S. (1999). Human mammary epithelial cells rapidly exchange empty EGFR between surface and intracellular pools. *J. Cell Physiol.* **180**, 448-460.

Campochiaro, P. A., Hackett, S. F., Vinores, S. A., Freund, J., Csaky, C., Larochelle, W., Henderer, J., Johnson, M., Rodriguez, I. R., Friedman, Z. et al. (1994). Platelet-derived growth-factor is an autocrine growth stimulator in retinal pigmented epithelial-cells. *J. Cell Sci.* **107**, 2459-2469.

Carpenter, G. and Wahl, M. I. (1990). The epidermal growth factor family. In *Peptide Growth Factors and their Receptors*. Vol. 95 (ed. M. B. Sporn and A. B. Roberts), pp. 69-171. Berlin, New York, Heidelberg: Springer-Verlag.

Cook, P. W., Ashton, N. M., Karkaria, C. E., Siess, D. C. and Shipley, G. D. (1995). Differential-effects of a heparin antagonist (hexadimethrine) or chlorate on amphiregulin, basic fibroblast growth-factor, and heparin-binding EGF-like growth-factor activity. *J. Cell. Physiol.* **163**, 418-429.

Dempsey, P. J. and Coffey, R. J. (1994). Basolateral targeting and efficient

consumption of transforming growth factor-alpha when expressed in madin-darby canine kidney-cells. *J. Biol. Chem.* **269**, 16878-16889.

Dempsey, P. J., Meise, K. S., Yoshitake, Y., Nishikawa, K. and Coffey, R. J. (1997). Apical enrichment of human EGF precursor in Madin-Darby canine kidney cells involves preferential basolateral ectodomain cleavage sensitive to a metalloprotease inhibitor. *J. Cell Biol.* **138**, 747-758.

Derynck, R. (1992). The physiology of transforming growth factor-alpha. *Adv. Cancer Res.* **5**, 27-53.

Dimarco, E., Pierce, J. H., Fleming, T. P., Kraus, M. H., Molloy, C. J., Aaronson, S. A. and Difiore, P. P. (1989). Autocrine interaction between TGF-alpha and the EGF-receptor – quantitative requirements for induction of the malignant phenotype. *Oncogene* **4**, 831-838.

Dong, J. Y. and Wiley, H. S. (2000). Trafficking and proteolytic release of epidermal growth factor receptor ligands are modulated by their membrane-anchoring domains. *J. Biol. Chem.* **275**, 557-564.

Dong, J. Y., Opresko, L. K., Dempsey, P. J., Lauffenburger, D. A., Coffey, R. J. and Wiley, H. S. (1999). Metalloprotease-mediated ligand release regulates autocrine signaling through the epidermal growth factor receptor. *Proc. Natl. Acad. Sci. USA* **96**, 6235-6240.

Duprez, V., Lenoir, G. and Dautryvarsat, A. (1985). Autocrine growth-stimulation of a human T-cell lymphoma line by interleukin-2. *Proc. Natl. Acad. Sci. USA* **82**, 6932-6936.

Eisenkraft, B. L., Nanus, D. M., Albino, A. P. and Pfeffer, L. M. (1991). Alpha-interferon down-regulates epidermal growth-factor receptors on renal-carcinoma cells in relation to cellular responsiveness to the antiproliferative action of alpha-interferon. *Cancer Res.* **51**, 5881-5887.

Fan, H. and Derynck, R. (1999). Ectodomain shedding of TGF-alpha and other transmembrane proteins is induced by receptor tyrosine kinase activation and MAP kinase signaling cascades. *EMBO J.* **18**, 6962-6972.

Forsten, K. E. and Lauffenburger, D. A. (1992). Autocrine ligand-binding to cell receptors – mathematical-analysis of competition by solution decoys. *Biophy. J.* **61**, 518-529.

Forsten, K. E. and Lauffenburger, D. A. (1994). Probability of autocrine ligand capture by cell-surface receptors: implications for ligand secretion measurements. *J. Comput. Biol.* **1**, 15-23.

French, A. R., Sudlow, G. P., Wiley, H. S. and Lauffenburger, D. A. (1994). Postendocytic trafficking of epidermal growth factor-receptor complexes is mediated through saturable and specific endosomal interactions. *J. Biol. Chem.* **269**, 15749-15755.

French, A. R., Tadaki, D. K., Niyogi, S. K. and Lauffenburger, D. A. (1995). Intracellular trafficking of epidermal growth-factor family ligands is directly influenced by the pH sensitivity of the receptor-ligand interaction. *J. Biol. Chem.* **270**, 4334-4340.

Gechtman, Z., Alonso, J. L., Raab, G., Ingber, D. E. and Klagsbrun, M. (1999). The shedding of membrane-anchored heparin-binding epidermal-like growth factor is regulated by the Raf/mitogen-activated protein kinase cascade and by cell adhesion and spreading. *J. Biol. Chem.* **274**, 28828-28835.

Gill, G. N., Kawamoto, T., Cochet, C., Le, A., Sato, J. D., Masui, H., McLeod, C. and Mendelsohn, J. (1984). Monoclonal anti-epidermal growth factor receptor antibodies which are inhibitors of epidermal growth factor binding and antagonists of epidermal growth factor binding and antagonists of epidermal growth factor-stimulated tyrosine protein kinase activity. *J. Biol. Chem.* **259**, 7755-7760.

Golembo, M., Raz, E. and Shilo, B. Z. (1996). The Drosophila embryonic midline is the site of Spitz processing, and induces activation of the EGF receptor in the ventral ectoderm. *Development* **122**, 3363-3370.

Gossen, M. and Bujard, H. (1992). Tight control of gene-expression in mammalian-cells by tetracycline-responsive promoters. *Proc. Natl. Acad. Sci. USA* **89**, 5547-5551.

Hackel, P. O., Zwick, E., Prenzel, N. and Ullrich, A. (1999). Epidermal growth factor receptors: critical mediators of multiple receptor pathways. *Curr. Opin. Cell Biol.* **11**, 184-189.

Herbst, J. J., Opresko, L. K., Walsh, B. J., Lauffenburger, D. A. and Wiley, H. S. (1994). Regulation of postendocytic trafficking of the epidermal growth-factor receptor through endosomal retention. *J. Biol. Chem.* **269**, 12865-12873.

Higashiyama, S., Abraham, J. A., Miller, J., Fiddes, J. C. and Klagsbrun, M. (1991). A heparin-binding growth-factor secreted by macrophage-like cells that is related to EGF. *Science* **251**, 936-939.

Hioki, O., Minemura, M., Shimizu, Y., Kasii, Y., Nishimori, H., Takahara, T., Higuchi, K., Yoshitake, Y., Nishikawa, K. and Watanabe, A. (1996). Expression and localization of basic fibroblast growth factor (bFGF) in the repair process of rat liver injury. *J. Hepatol.* **24**, 217-224.

Jhappan, C., Stahle, C., Harkins, R. N., Fausto, N., Smith, G. H. and Merlino, G. T. (1990). TGF-alpha overexpression in transgenic mice induces liver neoplasia and abnormal-development of the mammary-gland and pancreas. *Cell* **61**, 1137-1146.

Kaech, S. M., Whitfield, C. W. and Kim, S. K. (1998). The LIN-2/LIN-7/LIN-10 complex mediates basolateral membrane localization of the C-elegans EGF receptor LET-23 in vulval epithelial cells. *Cell* **94**, 761-771.

Kim, H. G., Kassis, J., Souto, J. C., Turner, T. and Wells, A. (1999). EGF receptor signaling in prostate morphogenesis and tumorigenesis. *Histol. Histopathol.* **14**, 1175-1182.

Kim, S. K. (1997). Polarized signaling: basolateral receptor localization in epithelial cells by PDZ-containing proteins. *Curr. Opin. Cell Biol.* **9**, 853-859.

Kornfeld, K. (1997). Vulval development in *Caenorhabditis elegans*. *Trends Genet.* **13**, 55-61.

Kudlow, J. E. and Bjorge, J. D. (1990). TGF alpha in normal physiology. *Semin. Cancer Biol.* **1**, 293-302.

Lauffenburger, D. A., Oehrtman, G. T., Walker, L. and Wiley, H. S. (1998). Real-time quantitative measurement of autocrine ligand binding indicates that autocrine loops are spatially localized. *Proc. Natl. Acad. Sci. USA* **95**, 15368-15373.

Li, S. W., Plowman, G. D., Buckley, S. D. and Shipley, G. D. (1992). Heparin inhibition of autonomous growth implicates amphiregulin as an autocrine growth-factor for normal human mammary epithelial-cells. *J. Cell. Physiol.* **153**, 103-111.

Lund, K. A., Lazar, C. S., Chen, W. S., Walsh, B. J., Welsh, J. B., Herbst, J. J., Walton, G. M., Rosenfeld, M. G., Gill, G. N. and Wiley, H. S. (1990). Phosphorylation of the epidermal growth factor receptor at threonine 654 inhibits ligand-induced internalization and down-regulation. *J. Biol. Chem.* **265**, 20517-20523.

Massague, J. and Pandiella, A. (1993). Membrane-anchored growth-factors. *Annu. Rev. Biochem.* **62**, 515-541.

Matsui, Y., Halter, S. A., Holt, J. T., Hogan, B. L. M. and Coffey, R. J. (1990). Development of mammary hyperplasia and neoplasia in MMTV TGF-alpha transgenic mice. *Cell* **61**, 1147-1155.

McConnell, H. M., Owicki, J. C., Parce, J. W., Miller, D. L., Baxter, G. T., Wada, H. G. and Pitchford, S. (1992). The cytosensor microphysiometer – biological applications of silicon technology. *Science* **257**, 1906-1912.

Miettinen, P. J., Berger, J. E., Meneses, J., Phung, Y., Pedersen, R. A., Werb, Z. and Derynck, R. (1995). Epithelial immaturity and multiorgan failure in mice lacking epidermal growth-factor receptor. *Nature* **376**, 337-341.

Oehrtman, G. T., Wiley, H. S. and Lauffenburger, D. A. (1998). Escape of autocrine ligands into extracellular medium: experimental test of theoretical model predictions. *Biotechnol. Bioeng.* **57**, 571-582.

Opresko, L. K., Chang, C. P., Will, B. H., Burke, P. M., Gill, G. N. and Wiley, H. S. (1995). Endocytosis and lysosomal targeting of epidermal growth-factor receptors are mediated by distinct sequences independent of the tyrosine kinase domain. *J. Biol. Chem.* **270**, 4325-4333.

Pandiella, A. and Massague, J. (1991). Multiple signals activate cleavage of the membrane transforming growth factor-alpha precursor. *J. Biol. Chem.* **266**, 5769-5773.

Peschon, J. J., Slack, J. L., Reddy, P., Stocking, K. L., Sunnarborg, S. W., Lee, D. C., Russell, W. E., Castner, B. J., Johnson, R. S., Fitzner, J. N. et al. (1998). An essential role for ectodomain shedding in mammalian development. *Science* **282**, 1281-1284.

Piepkorn, M., Pittelkow, M. R. and Cook, P. W. (1998). Autocrine regulation of keratinocytes: the emerging role of heparin-binding, epidermal growth factor-related growth factors. *J. Invest. Dermatol.* **111**, 715-721.

Russell, W. E., Dempsey, P. J., Sitaric, S., Peck, A. J. and Coffey, R. J. (1993). Transforming growth-factor-alpha (TGF-alpha) concentrations increase in regenerating rat-liver – evidence for a delayed accumulation of mature TGF-alpha. *Endocrinology* **133**, 1731-1738.

Sandgren, E. P., Luetteke, N. C., Palmiter, R. D., Brinster, R. L. and Lee, D. C. (1990). Overexpression of TGF-alpha in transgenic mice – induction of epithelial hyperplasia, pancreatic metaplasia, and carcinoma of the breast. *Cell* **61**, 1121-1135.

Shing, Y., Christofori, G., Hanahan, D., Ono, Y., Sasada, R., Igarashi, K. and Folkman, J. (1993). Betacellulin – a mitogen from pancreatic beta-cell tumors. *Science* **259**, 1604-1607.

Shoyab, M., Plowman, G. D., McDonald, V. L., Bradley, J. G. and Todaro, G. J. (1989). Structure and function of human amphiregulin – a member of the epidermal growth-factor family. *Science* **243**, 1074-1076.

Sibilia, M. and Wagner, E. F. (1995). Strain-dependent epithelial defects in mice lacking the EGF receptor. *Science* **269**, 234-238.

Sporn, M. B. and Roberts, A. B. (1992). Autocrine secretion – 10 years later. *Ann. Intern. Med.* **117**, 408-414.

Sporn, M. B. and Todaro, G. J. (1980). Autocrine secretion and malignant transformation of cells. *New Engl. J. Med.* **303**, 878-880.

Thompson, S. A., Higashiyama, S., Wood, K., Pollitt, N. S., Damm, D., McEnroe, G., Garrick, B., Ashton, N., Lau, K., Hancock, N. et al. (1994). Characterization of sequences within heparin-binding EGF-like growth-factor that mediate interaction with heparin. *J. Biol. Chem.* **269**, 2541-2549.

Threadgill, D. W., Dlugosz, A. A., Hansen, L. A., Tennenbaum, T., Lichti, U., Yee, D., Lamantia, C., Mourton, T., Herrup, K., Harris, R. C. et al. (1995). Targeted disruption of mouse EGF receptor – effect of genetic background on mutant phenotype. *Science* **269**, 230-234.

Toyoda, H., Komurasaki, T., Uchida, D., Takayama, Y., Isobe, T., Okuyama, T. and Hanada, K. (1995). Epiregulin – a novel epidermal growth-factor with mitogenic activity for rat primary hepatocytes. *J. Biol. Chem.* **270**, 7495-7500.

Valverius, E. M., Bates, S. E., Stampfer, M. R., Clark, R., McCormick, F., Salomon, D. S., Lippman, M. E. and Dickson, R. B. (1989). Transforming growth factor alpha production and epidermal growth factor receptor expression in normal and oncogene transformed human mammary epithelial cells. *Mol. Endocrinol.* **3**, 203-214.

Van de Vijver, M. J., Kumar, R. and Mendelsohn, J. (1991). Ligand-induced activation of A431 cell epidermal growth factor receptors occurs primarily by an autocrine pathway that acts upon receptors on the surface rather than intracellularly. *J. Biol. Chem.* **266**, 7503-8.

Wang, Y., Selden, A. C., Morgan, N., Stamp, G. W. H. and Hodgson, H. J. F. (1994). Hepatocyte growth factor/scatter factor expression in human mammary epithelium. *Am. J. Pathol.* **144**, 675-682.

Wiley, H. S., Herbst, J. J., Walsh, B. J., Lauffenburger, D. A., Rosenfeld, M. G. and Gill, G. N. (1991). The role of tyrosine kinase-activity in endocytosis, compartmentation, and downregulation of the epidermal growth-factor receptor. *J. Biol. Chem.* **266**, 11083-11094.

Wiley, H. S., Woolf, M. F., Opresko, L. K., Burke, P. M., Will, B., Morgan, J. R. and Lauffenburger, D. A. (1998). Removal of the membrane-anchoring domain of epidermal growth factor leads to intracrine signaling and disruption of mammary epithelial cell organization. *J. Cell Biol.* **143**, 1317-1328.

Will, B., Lauffenburger, D. A. and Wiley, H. S. (1995). Studies on engineering autocrine systems: requirements for ligand release from cells producing an artifical growth factor. *Tissue Eng.* **1**, 81-94.

Wojcik, S. F., Capen, C. C. and Rosol, T. J. (1999). Expression of PTHrP and the PTH PTHrP receptor in purified alveolar epithelial cells, myoepithelial cells, and stromal fibroblasts derived from the lactating rat mammary gland. *Exp. Cell Res.* **248**, 415-422.